J. Phys. D: Appl. Phys. 24 (1991) 1789–1795. Printed in the UK

On anode spots, double layers and plasma contactors

Bin Song, N D'Angelo and R L Merlino

Department of Physics and Astronomy, The University of Iowa, Iowa City, Iowa 52242-1479, USA

Received 7 March 1991, in final form 10 May 1991

Abstract. Luminous, sharply defined and nearly spherical objects ('fireballs'), typically several centimetres in diameter, have been observed in Ar, Kr and Xe plasmas. The 'fireballs' are anchored on a disk anode biased at 40–50 V above ground potential. They have been analysed in terms of a spherical double-layer model, in which ionization of the gas atoms by electrons energized at the double layer plays an essential role. The relevance is discussed of the present results to the so-called 'plasma contactors' to be used in space, especially in view of applications to electrodynamic tethers.

1. Introduction

Anode spots may occur when the current to the anode of a glow discharge is too small to maintain the discharge. Additional ionization can then be provided by electron–atom collisions near the anode and an electric field that energizes the electrons up to and above the ionization energy of the gas. Emeleus (1982) has given a review of anode glows in glow discharges and has discussed some of the problems still outstanding. Recent experiments on anode spots are also described by Seyhoonzadeh *et al* (1988).

Double layers have been investigated both experimentally (e.g. Torvén and Babić 1975, Quon and Wong 1976, Torvén and Andersson 1979, Cartier and Merlino 1987) and theoretically (e.g. Knorr and Goertz 1974, Goertz and Joyce 1975, DeGroot *et al* 1977, Borovsky and Joyce 1983) for a number of years. Double-layer research has also involved observations in space and several review papers have been published (e.g. Block 1978, Torvén 1979, Sato 1982, Hershkowitz 1985).

Plasma contactors have been discussed more recently as a means of establishing a low-impedance plasma bridge that can conduct current between a contactor electrode and a dilute plasma (e.g. Wilbur and Laupa 1988). The role of a contactor plasma appears to be particularly important from the point of view of electrodynamic tether applications where large currents must be drawn to electrodes of the upper or lower satellite. A recent paper by Gilchrist *et al* (1990) reports the observations of current collection enhancements due to nitrogen gas emission from a highly charged rocket payload in the ionosphere, when an electrically tethered mother/daughter system was used. The current enhancement is attributed to an electrical discharge that forms near positively charged vehicles by the release of the nitrogen gas.

In the present paper we describe an investigation of luminous, sharply defined, nearly spherical objects with typical diameters of 5–10 cm ('fireballs') that form in contact with a disk electrode of 3 cm diameter, biased at a positive voltage of 40–50 V and immersed in an unmagnetized Ar, Kr or Xe plasma produced by a hot filament discharge at a gas pressure in the range $\sim 10^{-4}$ Torr ($\sim 1.3 \times 10^{-2}$ Pa) $\lesssim P \lesssim 2 \times 10^{-3}$ Torr (2.6×10^{-1} Pa). The present study has clear connections with and relevance to all three lines of investigations referred to above, as will become apparent in the next sections.

Section 2 of the paper contains a brief description of the experimental set-up and of the diagnostics used. Section 3 presents the experimental results, while section 4 contains a discussion of them. Finally, section 5 contains the conclusions.

2. Experimental set-up

The observations were made in an unmagnetized plasma discharge chamber ~60 cm in diameter and ~100 cm in length. Typically argon gas was used, but several observations were also made in krypton or in xenon. The plasma was produced by biasing a set of tungsten filaments, hot enough to emit thermionic electrons, at −60 V relative to the (grounded) chamber walls.

The plasma density was on the order of $\sim 10^9$ cm^{-3}, the electron temperature $T_e \approx 2$ eV and the ion temperature $T_i \lesssim 0.2$ eV. The neutral gas pressure, P, for

0022-3727/91/101789+07$03.50

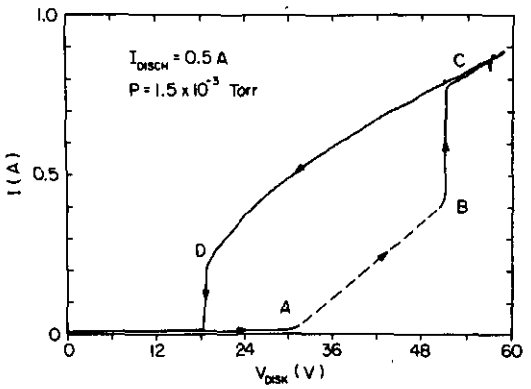

Figure 1. The *I* versus *V* characteristic of the 3 cm disk in an argon plasma. $P = 1.5 \times 10^{-3}$ Torr (2×10^{-1} Pa). In the A to B portion (broken line) the current was not steady, but consisted of spikes regularly spaced.

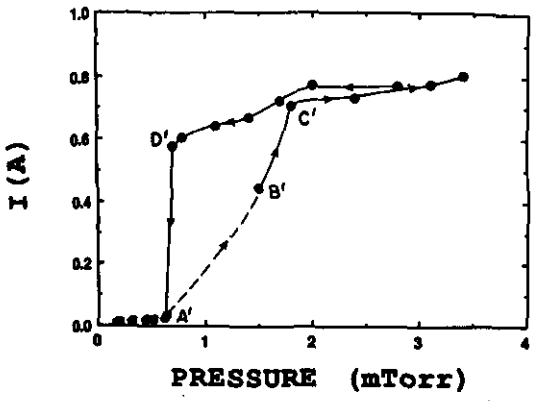

Figure 2. The *I* versus *P* characteristic of the 3 cm disk in an argon plasma. $V_{disk} \simeq +55$ V. In the A′ to B′ portion (broken line) the current consisted of regularly spaced spikes. As the pressure was varied, the discharge current was kept at a constant value of 2 A.

the set of experiments described here, was generally in the range 10^{-4} Torr (1.3×10^{-2} Pa) $\leqslant P \lesssim 2 \times 10^{-3}$ Torr (2.6×10^{-1} Pa). The diagnostic tools were Langmuir probes, for measurements of plasma density and electron temperature, and emissive probes to measure space potentials. The Langmuir probes consisted of flat tantalum disks of 3 mm diameter, while the emissive probes were made of tungsten wire, 0.1 mm in diameter and 3 mm in length, heated to emission by a direct current of ~2 A. In addition to the Langmuir probe and emissive probe measurements, visual observation of the 'fireballs' were made and colour photographs of them taken under several different sets of conditions.

The 'fireballs' were produced by biasing at a positive potential of 40–50 V, relative to the chamber wall, a metal disk of 3 cm diameter, coated on one side with a thin layer of nonconducting material. The external circuit consisted of a low-impedance power supply. The 3 cm diameter disk was supported by a long conducting wire covered with a non-conducting ceramic sleeve, and was located near the centre of the chamber, in front of an observation port.

3. Experimental results

We begin this section by showing in figure 1 a current versus voltage characteristic of the 3 cm disk in an argon plasma. The pressure of the gas was in this case $P = 1.5 \times 10^{-3}$ Torr (2×10^{-1} Pa) and the plasma density $n \simeq 3 \times 10^{8}$ cm^{-3}.

As the voltage on the disk was increased from 0 V to ~ 30 V, the disk current increased somewhat, up to a value of ~ 10^{-2} A (at $V_{disk} = 30$ V). A further increase of the voltage to ~ 50 V produced a more pronounced current increase. This portion of the characteristic (A to B) is indicated in figure 1 by the broken line. The current was not steady but rather consisted of spikes, occurring with regularity, the time between successive spikes decreasing steadily as the disk voltage increased. At $V_{disk} \approx 50$ V a sudden jump in the current took place (B to C). A further increase of V_{disk} produced only a moderate increase of the current. As V_{disk} was decreased below 50 V, the characteristic followed the path indicated by C to D. In this portion of the characteristic, as for $V_{disk} > 50$ V, the current was steady with no spikes present. At a $V_{disk} \lesssim V_D \approx 22$ V the disk current suddenly returned to a level of ~ 10^{-2} A.

If, instead of varying the disk voltage, the gas pressure was varied at a fixed disk voltage, the *I* versus *P* curve shown in figure 2 was obtained.

As *P* was increased from very low values up to ~ 0.7×10^{-3} Torr (~ 0.9×10^{-1} Pa), the disk current increased to ~ 10^{-2} A. A further increase of the pressure produced a more pronounced increase of the current. This portion of the *I* versus *P* curve is indicated in figure 2 by the broken line (A′ to B′). Again, the current consisted here of a series of regular spikes, as for the A to B segment of figure 1. At gas pressures larger than *P*(B′), a further increase of the pressure produced first a sudden increase of the disk current (B′ to C′), followed by a more moderate increase beyond C′. As *P* was decreased below ~ 2×10^{-3} Torr (~ 2.6×10^{-1} Pa), the system followed the path indicated by C′ to D′. In this portion of the curve, as for $P \gtrsim 2 \times 10^{-3}$ Torr, the current to the disk was steady with no spikes present. At $P \approx 0.8 \times 10^{-3}$ Torr (~ 1×10^{-1} Pa) (point D′) the current suddenly returned to a level of ~ 10^{-2} A.

Evidently, the disk voltage and the gas pressure play similar roles in determining the current collected by the disk. This similarity extends to the visual phenomena to be described next.

At various points along the *I* versus *V* characteristic of the disk, visual observations (figure 3) revealed the following. With V_{disk} just above 30 V, a luminous, planar sheath was produced on the conducting side of the disk, with a thickness of, perhaps, 2–3 mm. Over the portion of the *I* versus *V* curve marked by the broken line, one could observe a diffuse luminosity extending as much as 15–20 cm from the disk. Finally, at $V_{disk} \gtrsim 50$ V, after the current jump from B to C, a nearly spherical

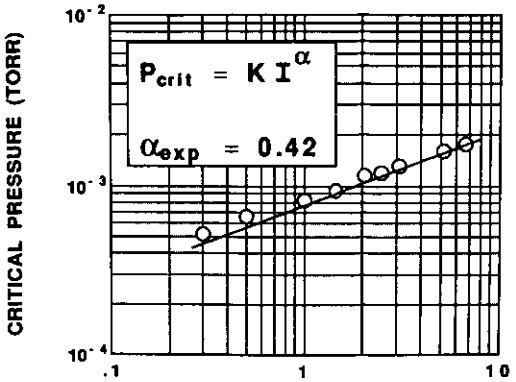

Figure 4. P_{crit} versus the plasma discharge current, for $V_{disk} = 40$ V (argon gas).

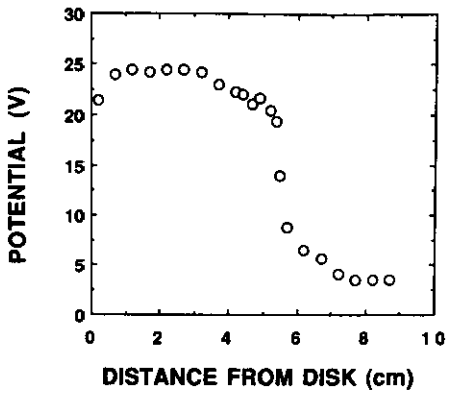

Figure 5. Profile of the space potential across a 'fireball' in argon ($P = 1.2 \times 10^{-3}$ Torr (1.6×10^{-1} Pa), $V_{disk} = 40$ V). The x-axis is perpendicular to the 3 cm disk through its centre, with $x = 0$ cm corresponding to the disk conducting surface.

intensely luminous region, with very sharply defined boundaries, was observed to be attached to the disk. Such a luminous object, which for brevity we call a 'fireball', persisted as V_{disk} was lowered from C to D. It then suddenly disappeared as V_{disk} was lowered below ~ 20 V.

A similar phenomenon was also observed when, instead of argon, we used either krypton or xenon gas.

Figure 3 shows colour photographs of (a) a luminous sheath attached to the 3 cm disk (argon gas), (*b*) a 'fireball' in argon and (*c*) a 'fireball' in krypton gas.

If, instead of varying the disk bias at a fixed value of the gas pressure, the disk bias was kept fixed at, say, $V_{disk} \simeq 40$–50 V, and the gas pressure was varied, it was observed that at relatively low gas pressure (A′ in figure 2) only a thin, planar, luminous sheath existed next to the disk. By increasing the pressure, a critical value, P_{crit}, would be reached slightly above which, suddenly, a 'fireball' developed (B′ in figure 2), which continued to be present at values of P several times as large as P_{crit}, although its size depended on the value of the pressure. Figure 4 shows, for argon gas, the variation of P_{crit} with the plasma discharge current (which is roughly proportional to the plasma density), for a fixed $V_{disk} = 40$ V. The data indicate a dependence of the type $P_{crit} = \text{const} \times I_{disk}^{\alpha}$ with $0.4 \lesssim \alpha \lesssim 0.5$.

A well-developed and stable 'fireball' can be studied by probing it with either an emissive probe or with a Langmuir probe. Figure 5 shows a profile of the space potential across a 'fireball' in argon, at $P = 1.2 \times 10^{-3}$ Torr (1.6×10^{-1} Pa) and $V_{disk} = 40$ V.

The x-axis is perpendicular to the 3 cm disk through its centre, with $x = 0$ cm corresponding to the disk's conducting surface. Evidently, a double layer is present near $x = 5.5$ cm, with a voltage difference between the inside of the 'fireball' and the surrounding plasma which is slightly in excess of the argon ionization potential (~ 16 V). Measurements within the 'fireball' indicate thermal electron densities several times larger than in the surrounding region.

An additional feature of 'fireballs' was studied, namely the dependence of their size on the pressure

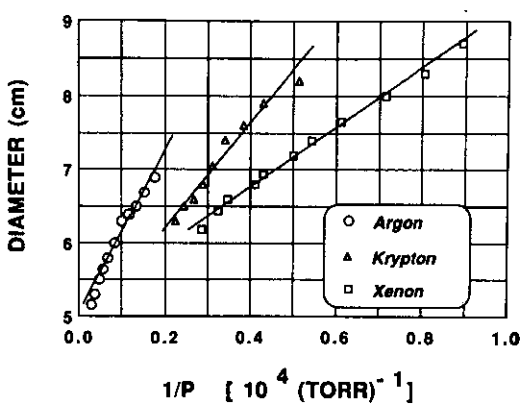

Figure 6. The 'fireball' diameter versus the inverse pressure, $1/P$, in Ar, Kr and Xe.

of the neutral gas and on the type of gas used. Figure 6 shows the 'fireball' diameter versus the inverse pressure, $1/P$, in Ar, Kr and Xe.

At the highest pressures the 'fireballs' attained their minimum size which, in the present experiment, was not smaller than about 5 cm. It is worth remembering that the diameter of the disk, to which a 'fireball' was anchored, was 3 cm and the diameter of a 'fireball' would be expected to be at least somewhat in excess of this.

Finally, if instead of the gas pressure the plasma density was varied, the 'fireball' diameter remained nearly constant, for a variation of the plasma density by as much as a factor ~ 7. However, when the plasma density was increased, there was a pronounced increase of the 'fireball' luminosity.

In figures 3 to 6 we have illustrated some of the properties of either the luminous sheaths or the 'fireballs' which are observed when the current to the disk is a *steady current*, on the order of $\sim 10^{-2}$ A for the luminous sheaths and of ~ 0.8 A for the 'fireballs'.

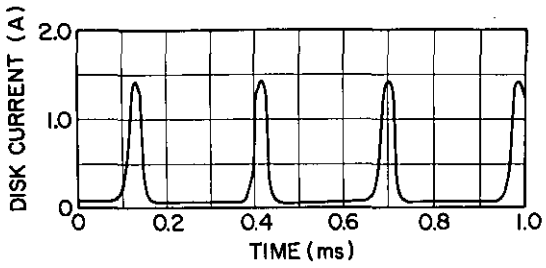

Figure 7. Disk current versus time, in the unstable regime (broken line of figure 1).

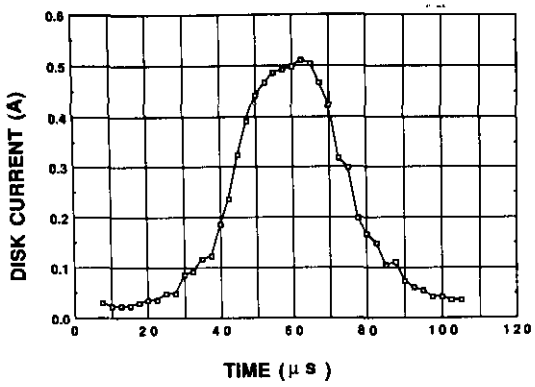

Figure 8. Disk current versus time, on an expanded time scale, in the unstable regime. Conditions are somewhat different from those in figure 7.

It is interesting, next, to provide a description of the behaviour of the system in the 'unstable' regime, namely the segment A to B of figure 1 or the segment A′ to B′ of figure 2. Figure 7 is a plot of the disk current versus time for such an unstable situation.

As already remarked, the current now consists of regularly spaced spikes. In the case of figure 7 the current spikes occur with a period of ~ 0.3 ms. One of these spikes, for somewhat different V_{disk} and gas pressure, is shown in figure 8 on an expanded time scale.

The disk current rises in this case to a peak value of ~ 0.5 A on a time scale of approximately 20 μs and decays in roughly the same time.

Time-resolved potential measurements in front of the disk were performed at different times during the current spike of figure 8. They are illustrated in figure 9, for times during which the current to the disk rises to its peak value of ~ 0.5 A, and in figure 10 as the disk current returns to its value of $\sim 10^{-2}$ A.

Evidently, as the current to the disk rises, a double-layer-like potential structure expands away from the disk into the surrounding plasma, while the potential of this plasma also rises from about -5 V to approximately $+12$ V. For times beyond the current peak, the potential difference between the main plasma and the region within a few centimetres from the disk falls below the gas ionization potential. Thus, the double-layer-like

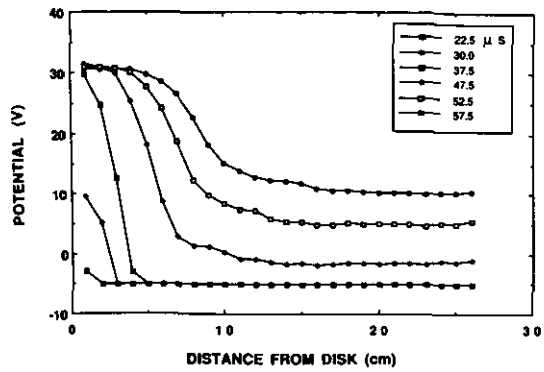

Figure 9. Time-resolved plots of the plasma potential in front of the disk, during the current rise in figure 8.

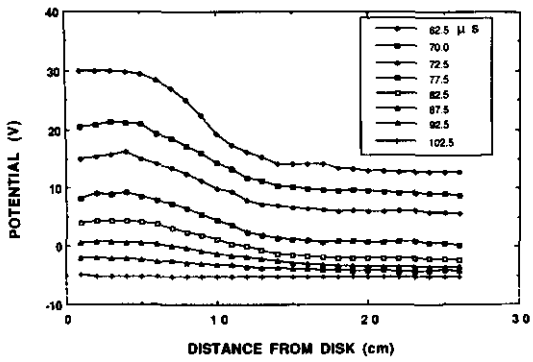

Figure 10. Time-resolved plots of the plasma potential in front of the disk, during the current fall in figure 8.

structure can no longer be maintained by ionization of the gas and must, therefore, retreat toward the disk.

It seems reasonable to suppose that the rise of the potential of the main plasma near the maximum of the current pulse is associated with a resistance between the plasma itself and the chamber walls. A variation of the plasma potential by ~ 20 V, when the current varies by ~ 0.5 A, suggests a plasma-to-wall resistance of $\sim 40\ \Omega$.

4. Discussion of the experimental results

In attempting to understand the experimental data of section 3, it is convenient to turn one's attention, first, to the luminous *anode sheath*, then to the conditions prevailing when a well-developed and stable spherical *double layer* is formed and, finally, to the relation between these two configurations and the evolution of one into the other as the gas pressure (or V_{disk}) is increased.

For the purposes of our discussion it is also convenient to reproduce here, as figure 11, curves of the ionization cross section, σ_i, for Ar, Kr and Xe obtained from the data of Rapp and Englander-Golden (1965).

At low gas pressure an invisible sheath exists next to the anode, whose thickness is on the order of several

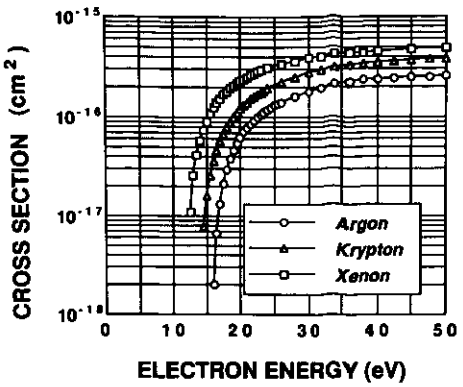

Figure 11. Ionization cross section, σ_i for Ar, Kr and Xe as a function of electron energy (from Rapp and Englander-Golden 1965).

Debye lengths. As the gas pressure is increased, ionization and excitation of neutral gas atoms within the sheath become important, and the sheath begins to become visible. As the sheath potential profile begins to be substantially modified to evolve into the stable double layer configuration, the ion density in the sheath n_{is} (which at lower pressures was entirely negligible) must be comparable to the electron density, n_{es}.

The rate of ion production in the sheath is

$$\sim n_{es}\left(\frac{eV_A}{m_e}\right)^{1/2}\delta\,\sigma_i(eV_A)\,N$$

where V_A is the (disk) anode voltage, δ the thickness of the sheath region where the potential is larger than the gas ionization potential, and N the neutral gas density. The ionization cross section $\sigma_i(eV_A)$ is to be computed at an electron energy on the order of eV_A, typically ~ 40 eV. The rate of ion loss from the sheath is

$$\sim n_{is}\left(\frac{eV_A}{m_i}\right)^{1/2}.$$

Balancing the ion loss with the ion production, and invoking the condition that $n_{is} \approx n_{es}$, we obtain

$$\left(\frac{m_i}{m_e}\right)^{1/2}\delta\,\sigma_i(eV_A)\,N \approx 1 \qquad (1)$$

which provides an estimate of δ. As an example, with $N \approx 3\times10^{13}$ cm^{-3}, $(m_i/m_e)^{1/2} \simeq 270$ (for argon) and σ_i (~ 40 eV) $\approx 2.6\times10^{-16}$ cm^2, we obtain $\delta \approx 0.5$ cm. This value of δ is somewhat larger than the 2–3 mm thickness observed for the luminous sheath, but still is of a comparable magnitude. The luminous sheath will likely appear somewhat thinner than our estimated δ, since most of the excitation of the neutral gas atoms in the sheath will occur close to the anode, where eV_A is substantially larger than the excitation energy. Also, since δ must be on the order of Debye lengths, equation (1) predicts that P_{crit} be proportional to the square root of the plasma density, consistent with the data in figure 4.

If we now turn to the stable double layer that forms at $P \gtrsim P_{crit}$, i.e. the 'fireball', we can write

$$\varphi_e\,D\,\sigma_i(\gtrsim E_{ion})N = \varphi_i \qquad (2)$$

where D is the 'fireball' diameter and φ_e and φ_i represent electron and ion fluxes, respectively, related by the usual Langmuir condition

$$\varphi_e = \left(\frac{m_i}{m_e}\right)^{1/2}\varphi_i\,. \qquad (3)$$

Equation (2) states that the rate of ion production within the 'fireball' must equal the rate of ion loss into the surrounding plasma. If we assume a double layer which is nearly spherically symmetric (except for the small region where the 'fireball' is attached to the anode), the total ion flux to the surrounding plasma is $4\pi(D/2)^2\varphi_i$, while the rate of ion production is, approximately, $4\pi(D/2)^2\varphi_e\,D\,\sigma_i(\gtrsim E_{ion})N$. The quantity $D\,\sigma_i(\gtrsim E_{ion})N$ is, of course, the ratio between an ionizing electron path length within the 'fireball', D, and the mean-free path for ionization, $1/[\sigma_i(\gtrsim E_{ion})N]$. This ratio represents the ionization probability per electron. Here, the cross section for ionization is to be evaluated at an energy only slightly above (by 1–2 eV) the ionization energy, since, as the experiment indicates, the voltage drop across the double layer is only marginally above the ionization potential of the gas. Referring to figure 11, we note that $\sigma_i(\gtrsim E_{ion})$ (see below) is only $\sim 0.1\sigma_i(40$ eV) or, possibly, even smaller. (2) and (3) can now be combined to yield

$$\left(\frac{m_i}{m_e}\right)^{1/2}D\,\sigma_i(\gtrsim E_{ion})N \approx 1\,. \qquad (4)$$

The values of $(m_i/m_e)^{1/2}$ and N used previously to estimate δ in argon, provide now a value of $D \gtrsim 5$ cm, which is on the order of the observed 'fireball' diameter. (4) predicts a 'fireball' diameter which increases with decreasing gas pressure and/or decreasing σ_i. The data in figure 6 are in general agreement with this prediction, when account is taken of the fact that the anode disk diameter was 3 cm (see section 3). In addition, (4) does not contain the density of the plasma surrounding the 'fireball', in agreement with the observation that the 'fireball' diameter is independent of the plasma density.

For a still more detailed comparison of (4) with observations, refer to figure 6, showing the 'fireball' diameter versus inverse pressure, $1/P$, for Ar, Kr and Xe. For each of the these gases consider the experimental point corresponding to the largest measured D, which, presumably, is the least affected by the finite anode disk diameter (3 cm). Applying (4) to these three points, we obtain the values of $\sigma_i(\gtrsim E_{ion})$ in Ar, Kr and Xe given in table 1. The values of σ_i in table 1 correspond, in each of the three gases, to an electron energy that is

Table 1. Values of σ_i in Ar, Kr and Xe.

Gas	σ_i (cm^2)
Argon	0.28×10^{-16}
Krypton	0.46×10^{-16}
Xenon	0.61×10^{-16}

about 2 eV above the ionization energy, as we argued above that it should be the case.

Finally, a few more comments are in order as to the transition from an anode sheath to a stable double-layer configuration. This is the regime indicated by dotted lines in the I versus V_{disk} curve of figure 1 or in the I versus P curve of figure 2.

Evidently, a sufficiently large disk voltage and/or a sufficiently large gas pressure are required for the system to be able to settle in the 'fireball' state. When either V_{disk} or P only marginally satisfy this condition, the system attempts to produce the 'fireball' state, but is unable to 'lock' into it permanently. Then we observe the current spikes of figure 7 and of figure 8, with the potential evolution illustrated in figure 9 and in figure 10. Presumably, as was briefly stated at the end of section 3, this inability of the system to settle permanently in the 'fireball' state is related to the general potential rise that takes place within the main plasma at or near the time of the disk current peak. This rise lowers the potential difference across the double-layer-like structures of figure 9 and figure 10 to less than the ionization potential of the gas. An increase of V_{disk}, on the other hand, circumvents this difficulty and assures the formation of a stable 'fireball'.

It is also of interest to relate the rise and fall time of the current in figure 8 to the production of ions by ionization and to their loss from the high-potential side of the double-layer-like structures into the surrounding plasma, respectively. The ionization time is given by

$$t_{ioniz} = \frac{1}{N\sigma_i v_e}$$

and, for the conditions of figure 8, is easily estimated to be some 10–20 μs, comparable to the current rise time. The loss time of the ions is also of the same order. What is less clear is what determines the repetition frequency of the current pulses in figure 7. At the end of a current pulse, we expect the ion density in the sheath to be much less than the electron density. On the other hand, at the beginning of the next pulse we must have this situation reversed, with $n_{is} \gtrsim n_{es}$, so that a double-layer-like structure will begin to develop. Then, the time between current pulses may simply be the time necessary for this reverse to take place, which may be on the order of many ionization times. That the pulse repetition frequency is probably related to the ionization time, is also suggested by the fact that this frequency increases with increasing disk voltage and increasing gas pressure. Note that

$$f_{ioniz} = \frac{1}{t_{ioniz}} = N\sigma_i v_e$$

exhibits the same behaviour.

The behaviour of an anode sheath in the presence of ionization has been studied numerically by Cooke and Katz (1988). The evolution of an anode sheath into a double layer, in the presence of ionization, has also been discussed by Andersson (1981) and Andersson and Sorensen (1983). Their calculations suggest that oscillations in the anode sheath must be taken into account to explain the transition to a double layer.

5. Conclusions

We have reported in this paper the observation of luminous, sharply defined and nearly spherical objects ('fireballs'), typically of many centimetres in diameter, which form on a disk anode biased at $\approx +40$ V relative to the walls of a chamber in which Ar, Kr or Xe plasmas are first produced by hot filament discharges. A typical observation reveals that, at fixed disk voltage, a gas pressure increase produces first a luminous, flat sheath of 2–3 mm thickness, which then 'explodes', with a further pressure increase, into a steady 'fireball'. The latter has been analysed in terms of a spherical double layer and a comparison has been made between a simple double-layer model and the observations.

It has been observed that the formation of the 'fireball' greatly increases the current collection capability of the disk anode. Data such as those in figure 1 indicate that current collection can easily be increased by a factor ~50, or more. This result is important from the point of view of the so-called 'plasma contactors' to be used in space, particularly in view of applications to electrodynamic tethers (e.g. Gilchrist *et al* 1990). As discussed, e.g., by Wilbur and Laupa (1988), plasma contactors and 'plumes' are essential in establishing low-impedance bridges that can conduct current between electrodes in the upper or lower satellite of a tether set-up and a tenuous ionospheric plasma.

Acknowledgment

Work supported by ONR and NASA.

References

Andersson D 1981 *J. Phys. D: Appl. Phys.* **14** 1403
Andersson D and Sorensen J 1983 *J. Phys. D: Appl. Phys.* **16** 601
Block L P 1978 *Astrophys. Space Sci.* **55** 59
Borovsky J E and Joyce G 1983 *J. Geophys. Res.* **88** 3116
Cartier L S and Merlino R L 1987 *Phys. Fluids* **30** 2549
Cooke D L and Katz I 1988 *J. Spacecr. Rockets* **25** 132
Emeleus K G 1982 *Int. J. Electronics* **52** 407
DeGroot J S, Barnes C, Walstead A E and Buneman O 1977 *Phys. Rev. Lett.* **38** 1283
Gilchrist B E, Banks P H, Neubert T, Williamson P R, Myers N B, Raitt W J and Sasaki S 1990 *J. Geophys. Res.* **95** 2469
Goertz C K and Joyce G 1975 *Astrophys. Space Sci.* **32** 165
Hershkowitz N 1985 *Space Sci. Rev.* **41** 351

Knorr G and Goertz C K 1974 *Astrophys. Space Sci.* **31** 209
Quon B H and Wong A Y 1976 *Phys. Rev. Lett.* **31** 1393
Rapp D and Englander-Golden P 1965 *J. Chem. Phys.* **43** 1464
Sato N 1982 *Proc. 1st Symp. on Plasma Double Layers (Risø)* ed P Michelsen and J J Rasmussen p 116
Seyhoonzadeh A, Forsling P, Bailey M, Rosario R, Beardsley K, Tao J and Lonngren K E 1988 *Phys. Fluids* **31** 682
Torvén S 1979 *Wave and Instabilities in Space Plasmas* ed P J Palmadesso and K Papadopoulos (Dordrecht: Reidel) p 109
Torvén S and Andersson D 1979 *J. Phys. D: Appl. Phys.* **12** 717
Torvén S and Babić M 1975 *Proc. 12th Int. Conf. on Phenomena in Ionized Gases* ed J G A Hölscher and D C Schram (Amsterdam: North-Holland) p 124
Wilbur P J and Laupa T G 1988 *Adv. Space Res.* **8** 221